Interfacial phenomena related to the fabrication of thin Al oxide tunnel barriers and their thermal evolution

T. Dimopoulos,[a] V. Da Costa, C. Tiusan, and K. Ounadjela
Institut de Physique et Chimie des Matériaux de Strasbourg (IPCMS), 23 rue du Loess, F-67037 Strasbourg Cedex, France

H. A. M. van den Berg
Siemens AG, ZT MF1, Paul Gossenstrasse 100, Erlangen D-91052, Germany

(Received 9 May 2001; accepted for publication 21 August 2001)

In this work we study phenomena related to the plasma oxidation of thin metallic Al layers, to be used as insulating barriers in magnetic tunnel junctions. We investigate by barrier impedance scanning microscopy how the barrier's over oxidation influences the local transport characteristics of the oxide layers and the results are correlated with the magnetotransport properties of patterned microsized as-deposited and annealed junctions. Interestingly, the *oxygen reservoir* existing at the ferromagnetic metal, degenerating the tunnel device, can be utilized for the improvement of the junction's magnetotransport properties by means of thermal annealing processing. © *2001 American Institute of Physics.* [DOI: 10.1063/1.1410361]

Following the discovery of large tunnel magnetoresistance (TMR) at room temperature,[1] magnetic tunnel junctions (MTJs) have been proved strong candidates for applications like sensors, magnetic random access memories and heads. Despite the use of state of the art thin film technology, and the increasing "know how" for the realization of ferromagnetic (FM) metal/oxide/FM metal MTJs, many problems are encountered. One of these concerns how thin the oxide barrier (usually alumina) can be and still maintaining high quality tunnel transport. As the need for thinner oxides (low resistive junctions) grows bigger, for applications like magnetic heads, usual oxidation techniques prove to be inadequate to secure self-limiting oxidation and, thus, sharp FM metal/oxide interfaces.

This letter investigates the influence of the FM metal/aluminum oxide interface quality, focusing on over oxidation effects on the junction's tunneling profile, analyzed using barrier impedance scanning microscopy (BISM)[2] and magnetotransport measurements of as-deposited and annealed patterned junctions (TMR and $I-V$ curves).

The multilayers were sputtered on Si wafers. Initially, a buffer trilayer of Cr(1.8 nm)/Fe(6 nm)/Cu(30 nm) is deposited. Upon the buffer, an artificial antiferromagnet (AAF) of $Co_{50}Fe_{50}$(1.5 nm)/Ru(0.8 nm)/$Co_{50}Fe_{50}$(2.7 nm) serves as the magnetically hard subsystem.[3,4] The barrier formation follows with the sputtering of a metallic Al film and subsequently oxidizing it within a rf Ar/O_2 plasma.[5] The magnetically soft electrode of $Co_{50}Fe_{50}$(1 nm)/Fe(6 nm) is deposited on the top of the barrier. Finally, the multilayer stack is capped with Cu(10 nm)/Cr(5 nm). UV photolithography is used to pattern the junctions in nominal areas of 3×3 up to $20\times20\ \mu m^2$. The transport measurements are realized with a four-point technique. The scaling of the resistance inversely with the area of the junction, the almost constant TMR regardless the junction's size and the low resistivity of the bottom Cu electrode ($<0.3\ \Omega$) exclude the possibility of geometrical enhancement of the TMR due to inhomogeneous current flow through the junction area.[6]

Tunnel junctions with different barrier thicknesses have been studied, as presented in Table I. Measurement of the AAF's net magnetic moment (Fig. 1) for the multilayers employing the barriers shown in Table I reveal that the oxidation of the CoFe electrode becomes more important for thinner Al films, causing the observed decrease of the net AAF's magnetic moment (Fig. 1). The continuity of the Al layer down to 6 Å of thickness is verified by transmission electron microscopy (TEM). The coverage of the FM metal surface with Al is not complete for 5 Å Al thickness, leading to a subsequent profound oxidation of CoFe, as clearly observed by TEM. We have to note here that prior to oxidation, the CoFe/Al interface is only slightly intermixed due to the chemical stability of the CoFe alloy[7] and the low kinetic energy of the sputtered Al (Al deposition rate <0.2 Å/s). The interfacial degradation is thus directly related to the subsequent oxidation process.

In the present study, the as-deposited junctions present a TMR signal ranging from ~25%, for 12 and 10 Å Al thickness, down to ~7% for 6 Å Al (TMR is almost nil for system *S*5), depending on the oxygen contamination of the FM electrode (see Table I). The $I-V$ curves are fitted to Brinkman's model.[8] For the thin barriers with imperfect interfaces studied here, the values of the barrier height and width extracted from the Brinkman model, and shown in Table I, can only be

TABLE I. Studied barriers and their magnetotransport properties.

	Al (Å)	$t_{ox}(s)$	$R\times A$ $k\Omega\times\mu m^2$	d (Å)	φ (eV)	$\langle i/i_{typ}\rangle$	TMR (%)
*S*1	12	45	35	9.7	2.2	1.2	24
*S*2	10	35	5.9	10.4	1.3	1.1	25.5
*S*3	8	35	1.4	11.7	0.75	2.3	14
*S*4	6	30	0.2	⋯	⋯	3	7
*S*5	5	30	0.3	⋯	⋯	10	0.6

[a]Electronic mail: thdimop@ipcms.u-strasbg.fr

 © 2001 American Institute of Physics
Downloaded 15 Feb 2006 to 194.214.217.17. Redistribution subject to AIP license or copyright, see http://apl.aip.org/apl/copyright.jsp

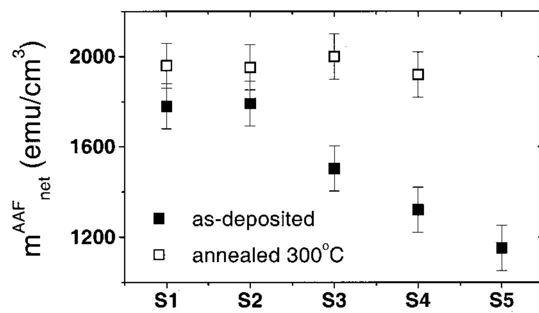

FIG. 1. The net magnetic moment of the AAF for the as-deposited and annealed multilayers employing the barriers under study.

treated as *apparent* values, which integrate all nonlinear transport mechanisms which exist in parallel with pure tunneling. The apparent barrier height decreases significantly when decreasing the metallic Al thickness prior to oxidation, from 2.2 down to 0.75 eV. Moreover, the barrier width, extracted from the fitting, seems to increase as the Al layer becomes thinner. The lowered apparent barrier height and the increased width can be attributed to the existence of an additional, small height, in cascade CoFe oxide originating from the over oxidation of the Al film.[9] Moodera *et al.*[10] have studied the evolution of TMR as a function of the Al film thickness for a given oxidation condition and found that an optimum Al thickness regime exists in order to avoid over or under oxidation effects. The results are comparable to the TMR values found in this study. Though, as we will show in the following paragraphs, the combination of local transport measurements with those made on patterned junctions brings further information on the mechanisms degrading the spin dependent transport in tunnel devices.

The oxygen contamination of the CoFe layer leads to an enhanced FM metal/oxide interfacial roughness, noncorrelated with the upper interface, originating from the mixing of metallic Fe and Co with their oxide compounds. Strong electronic scattering can be expected at such an interface, that causes local variations of conductance and of spin polarization.[11] In other words, electrons are considered to tunnel through potential barriers in parallel, with different height and/or thickness. To witness these local transport variations we need a technique which can spatially resolve the tunnel current in the nanometric scale. For this we have used BISM. This utilizes a conducting atomic force microscopy tip (commercial Si_3N_4 contact mode tip covered with 30 nm of TiN_x) to simultaneously acquire the topographic and the current map image of the scanned Al oxide surface, when a bias voltage (typically 1.5 V) is applied between the tip and the metallic electrode beneath the oxide.[2]

All barriers have been analyzed using this technique. The scanned images correspond to $500\times500\,\mathrm{nm}^2$ size areas (512×512 pixels). From the current map images, the probability distribution of the current was calculated (Fig. 2). We will call the most probable value of the current i_{typ}. Topographic profiles of the scanned areas show that all structures have comparable roughness values ($\sim$1 Å rms), showing no significant correlation with the current map images. In Fig. 2 we plot the normalized probability distribution for the quantity i/i_{typ} for all tunnel barriers. We use the quantity i/i_{typ} instead of i, in order to compare the statistical distributions in the same scale and to exclude any possibility of artifacts that may arise from the conducting tip from sample to sample. The log-normal type of the distributions is in agreement with the model provided in Refs. 12 and 13, which begins from the assumption that a Gaussian distribution of the barrier height or thickness exists for the studied oxide.

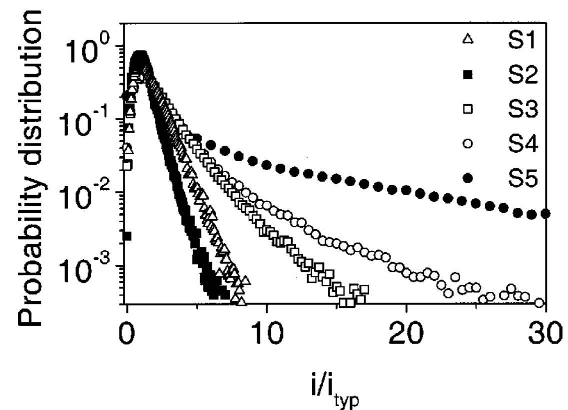

FIG. 2. Probability distribution curves for the local current, acquired by BISM.

Interestingly, the probability distribution broadens as the barrier becomes thinner, while its tail extends to higher i/i_{typ} values (Fig. 2). The mean value $\langle i/i_{\mathrm{typ}}\rangle$ is of particular importance as it characterizes the homogeneity of the tunnel barriers in patterned junctions. For higher disorder the position of the $\langle i/i_{\mathrm{typ}}\rangle$ value is shifted far away from the distribution maximum (a system without any fluctuations would show $\langle i/i_{\mathrm{typ}}\rangle=1$). Calculating $\langle i/i_{\mathrm{typ}}\rangle$ for each case, we get values ranging from 1.1 for Al 10 Å to 10 for Al 5 Å, as reported in Table I. The larger the deviation from unity the more significant is the contribution of the highly conducting sites (hot spots) of the distribution tail to the average current. We note here that in no case did the BISM experiment show existence of pinholes. Even the highest conducting sites, when probed by the tip, gave a nonlinear $I-V$ characteristic.

In the previous paragraphs we have attributed the degradation of the TMR values to the barrier over oxidation. It is thus reasonable to assume that by transferring the interfacial oxygen towards the barrier, by means of annealing, improvement of the magnetotransport properties of the junctions can be expected.[14] Moreover, this improvement should depend on the extent of the barrier's over oxidation. We have thermally treated several MTJ systems. We will at this point

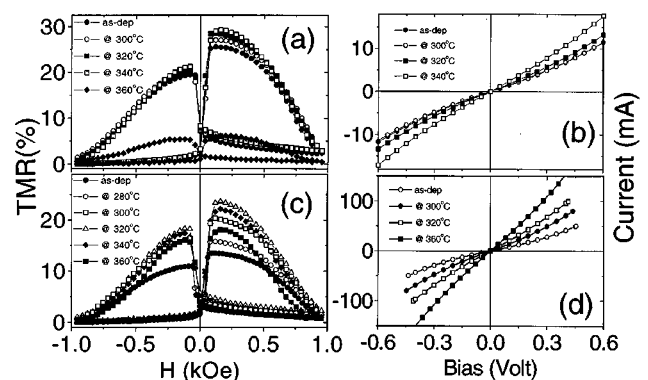

FIG. 3. TMR and $I-V$ curves for the system $S2$ [(a) and (b)] and system $S3$ [(c) and (d)], for characteristic annealing temperatures.

Downloaded 15 Feb 2006 to 194.214.217.17. Redistribution subject to AIP license or copyright, see http://apl.aip.org/apl/copyright.jsp

TABLE II. Evolution of junction parameters for systems $S2$ and $S3$ upon annealing.

T (°C)	$R\times A$ $k\Omega\times\mu m^2$		ϕ (eV)		d (Å)		TMR (%)	
	$S2$	$S3$	$S2$	$S3$	$S2$	$S3$	$S2$	$S3$
as-dep	5.9	1.37	1.3	0.75	10.4	11.7	25.6	14.0
@260	7.5	1.37	1.4	0.75	10.4	11.6	27.0	15.7
@280	7.4	1.15	1.4	0.80	10.4	11.2	27.1	15.9
@300	7.1	0.72	1.4	0.85	10.2	10.5	26.9	20.4
@320	6.1	0.47	1.5	1.00	9.8	9.5	28.6	23.7
@340	4.4	0.33	1.7	0.90	9.0	9.5	29.3	22.2
@360	1.0	0.31	⋯	0.85	⋯	8.8	6.2	18.1

consider two systems in particular: $S2$(10 Å Al) and $S3$(8 Å Al) annealed in the temperature range from 260 to 360 °C, with steps of 20 °C and 45 min annealing time at each temperature. We have already reported the differences of these two systems in terms of over oxidation (Fig. 1). Figure 3 presents the TMR and $I-V$ curves for the as-deposited and annealed states for $S2$ [Figs. 3(a) and 3(b)] and $S3$ [Figs. 3(c) and 3(d)] and for characteristic temperatures. The general trends concerning barrier parameters and TMR amplitude are summarized in Table II. The observed increase of the TMR with annealing, for both systems, is accompanied by an increase of the barrier height and a decrease in the barrier thickness. Interestingly, the relative changes, especially on the TMR, are more pronounced in the case of $S3$, for which the CoFe layer is more affected by oxidation. Given adequate thermal activation energy, oxygen moves from the FM electrode towards the barrier, due to its larger affinity for Al, improving the Al oxide's stoichiometry. The temperature at which the oxygen transfer occurs can be determined from the evolution of the junction's resistance with annealing, as this is driven by the interplay between the barrier height, which increases with annealing and the barrier width, which decreases when in-cascade "barriers" are annihilated. For instance, this occurs at 340 °C for $S2$ and at 320 °C for $S3$. The annihilation of the CoFe oxide is further confirmed by the recovery of the net AAF's magnetic moment, which occurs at the same temperature range for the annealed multilayers (Fig. 1). At higher annealing temperatures (above 340 °C) intermixing processes lead to the degradation of the barrier at localized sites, lowering the TMR value drastically.

We believe that the concept of the *oxygen reservoir* is very important for a large MR ratio. Purposely over oxidizing the Al to create this oxygen reservoir allows us to improve the stoichiometry of the barrier upon annealing. This has been done on junctions with identical Al thicknesses (12 Å) and different oxidation times (40 and 45 s). The results show that for the over oxidized junction, indeed the MR is lower for the as-deposited state—24%—compared to the optimized oxidized junction—30%—while after annealing the MR increases drastically to 39% for the former and to 33% for the latter.

In conclusion, we have shown using local transport measurements that over oxidized thin Al oxide barriers present an inhomogeneous tunnel current profile. Current hot spots related to low barrier height and/or width are at the origin of the degradation of the magnetotransport properties of patterned magnetic tunnel junctions. Most importantly, the presence of FM metal oxide at the interface with the barrier can be advantageous for the junction's spin dependent transport profile after thermal anneal processing.

The authors would like to thank Dr. Y. Henry, Dr. J. Hommet, G. Ehret, M. Acosta, G. Wurtz, Dr. C. Meny, and Dr. L. Bäer for experimental support. This work was partially supported by the European Community Brite Euram project "Tunnelsense" (BRPR98-0657) and the Training and Mobility of Researchers program of the EC through the "Dynaspin" project (FMRX-CT97-0124).

[1] J. S. Moodera, L. R. Kinder, T. M. Wong, and R. Meservey, Phys. Rev. Lett. **74**, 3273 (1995).
[2] V. da Costa, C. Tiusan, T. Dimopoulos, and K. Ounadjela, Phys. Rev. Lett. **85**, 876 (2000).
[3] H. A. M. van den Berg, W. Clemens, G. Gieres, G. Rupp, M. Vieth, J. Wecker, and S. Zoll, J. Magn. Magn. Mater. **165**, 524 (1997).
[4] C. Tiusan, T. Dimopoulos, K. Ounadjela, M. Hehn, H. A. M. van den Berg, Y. Henry, and V. Da Costa, Phys. Rev. B **61**, 580 (2000).
[5] J. Nassar, M. Hehn, A. Vaures, F. Petroff, and A. Fert, Appl. Phys. Lett. **73**, 698 (1998).
[6] J. S. Moodera, L. R. Kinder, J. Nowak, P. LeClair, and R. Meservey, Appl. Phys. Lett. **69**, 708 (1996).
[7] T. Dimopoulos, C. Tiusan, V. da Costa, K. Ounadjela, and H. A. M. van den Berg, Appl. Phys. Lett. **77**, 3624 (2000).
[8] W. F. Brinkman, R. C. Dynes, and J. M. Rowell, J. Appl. Phys. **41**, 1915 (1970).
[9] H. Brückl, J. Schmalhorst, G. Reiss, G. Gieres, and J. Wecker, Appl. Phys. Lett. **78**, 1113 (2001).
[10] J. S. Moodera, E. F. Gallagher, K. Robinson, and J. Nowak, Appl. Phys. Lett. **70**, 3050 (1997).
[11] A. Vedyayev, N. Ryzhanova, R. Vlutters, and B. Dieny, Europhys. Lett. **46**, 808 (1999).
[12] F. Bardou, Europhys. Lett. **39**, 239 (1997).
[13] V. da Costa, Y. Henry, F. Bardou, M. Romeo, and K. Ounadjela, Eur. Phys. J. B **13**, 297 (2000).
[14] R. C. Sousa, J. J. Sun, V. Soares, P. P. Freitas, A. Kling, M. F. da Silva, and J. C. Soares, Appl. Phys. Lett. **73**, 3288 (1998).

Downloaded 15 Feb 2006 to 194.214.217.17. Redistribution subject to AIP license or copyright, see http://apl.aip.org/apl/copyright.jsp